Received: 25 August 2016 | Accepted: 22 February 2017

DOI: 10.1002/hyp.11156

WILEY

RESEARCH ARTICLE

The influence of lithology on surface water sources

Lydia B. Nickolas[1,2] | Catalina Segura[1,2] | J. Renée Brooks[3]

[1] Forest Engineering, Resources, and Management, Oregon State University, Corvallis, OR, USA

[2] Water Resources Graduate Program, Oregon State University, Corvallis, OR, USA

[3] Western Ecology Division, National Health and Environmental Effects Research Laboratory, U.S. Environmental Protection Agency, Corvallis, OR, USA

Correspondence
Catalina Segura, Forest Engineering, Resources, and Management, Oregon State University, 201 Peavy Hall, Corvallis, OR 97331, USA.
Email: catalina.segura@oregonstate.edu

Funding Information
H.J. Andrews Experimental Forest LTER7, Grant/Award Number: 1440409; USDA National Institute of Food and Agriculture; McIntire Stennis project OREZ-FERM-876; Department of Forestry Engineering Resources and Management at Oregon State University (OSU)

Abstract

Understanding the temporal and spatial variability of water sources within a basin is vital to our ability to interpret hydrologic controls on biogeochemical processes and to manage water resources. Water stable isotopes can be used as a tool to determine geographic and seasonal sources of water at the basin scale. Previous studies in the Coastal Range of Oregon reported that the variation in the isotopic signatures of surface water did not conform to the commonly observed "elevation effect," which exhibits a trend of increasing isotopic depletion with rising elevation. The primary purpose of this research is to investigate the mechanisms governing seasonal and spatial variations in the isotopic signature of surface waters within the Marys River Basin, located in the leeward side of the Oregon Coastal Range. Surface water and precipitation samples were collected every 2–3 weeks for isotopic analysis for 1 year. Our results confirmed the lack of elevational variation of surface water isotopes within this leeward basin. Although we find elevational variation in precipitation in the eastern portion of the watershed, this elevation effect is counteracted by rainout with distance from the Pacific coast. In addition, we found significant variation in surface water isotope values between catchments underlain predominantly by basalt or sandstone. The degree of separation was strongest during the summer when low flows reflect deeper groundwater sources. This indicates that baseflow within streams drained by each lithology is being supplied from two distinctly separate water sources. In addition, the flow of the Marys River is dominated by water originating from the sandstone water source, particularly during the low-flow summer months. We interpreted that the difference in water source results from sandstone catchments having highly fractured geology or locally tipping to the east facilitating cross-basin water exchange from the windward to the leeward side of the Coast Range. Our results challenge topographic derived watershed boundaries in permeable sedimentary rocks; highlighting the overwhelming importance of underlying geology.

KEYWORDS

baseflow, Oregon Coast Range, elevation, lapse isotopic rate, lithology, source water, water isotopes

1 | INTRODUCTION

Understanding the spatial and temporal variability of stream water sources is vital to our ability to interpret hydrologic controls on biogeochemical processes and to manage water resources. Within relatively uniform watersheds, previous modeling efforts to extrapolate hydrologic behaviors from gauged to ungauged basins have greatly improved our understanding of controlling factors, thus increasing predictive capacity (McDonnell et al., 2007; McGuire et al., 2005; Parajka et al., 2013; Wagener & Montanari, 2011; Yadav, Wagener, & Gupta, 2007; Zhang, Wagener, Reed, & Bhushan, 2008). These gauged–ungauged modeling approaches indicate the strength of incorporating a priori parameter estimates of regional physical watershed characteristics (e.g., topography, geology, and slope) for improving estimations of streamflow within ungauged basins. For example, geology is a strong controlling factor on mean transit time. In Oregon, mean transit time in catchments draining volcanic rocks is correlated with terrain indices representing the flow path distance and flow path gradient to the stream network (McGuire et al., 2005), whereas drainage area scales with mean transit time in sandstone dominated catchments (Hale & McDonnell, 2016). Geology was also a controlling factor in the spatial variability of mean transit in an arid catchment in Arizona during saturated conditions (Heidbuchel, Troch, & Lyon, 2013). However, in watersheds with complex variable characteristics (e.g., geology and

climate), we still need approaches that capture localized variability in catchment attributes that may significantly affect seasonal and spatial variations in hydrologic flow paths and source contributions. For example, Patil, Wigington, Leibowitz, Sproles, and Comeleo (2014) found that spatially distributed climate data noticeably improved hydrological modeling in watersheds with high variability in climatic characteristics. Mixed lithology within a watershed still present challenges to understanding hydrologic behavior (Sprenger, Seeger, Blume, & Weiler, 2016). Thus, despite these advances in modeling for relatively homogenous watershed, significant strides must still be made in interpreting hydrologic behavior and source water variability within watersheds with complex characteristics.

Current approaches for identifying spatial and temporal variations in stream water sources are largely insufficient for understanding the effects of spatially heterogeneous catchment characteristics such as topography, geology, and land cover (Brooks, Wigington, Phillips, Comeleo, & Coulombe, 2012; Klaus & McDonnell, 2013; McGuire et al., 2005; Mountain, James, & Chutko, 2015). Conventional methods primarily rely upon nested stream gauges along the mainstem of the river and major tributaries; however, they fail to incorporate small tributaries and headwater streams, simultaneously. Consequently, our understanding of how these smaller (yet crucial) systems influence streamflow dynamics at the river basin scale is limited (Payn, Gooseff, McGlynn, Bencala, & Wondzell, 2012; Singh, Emanuel, & McGlynn, 2016). Additionally, due to resource limitations, most studies must choose to prioritize either spatially or temporally intensive sampling, which leads to an inability to concurrently interpret important seasonal and spatial variations. Although several studies have investigated variations in stream water source and surface water–groundwater interactions within small (<240 km^2) (Blumstock, Tetzlaff, Malcolm, Nuetzmann, & Soulsby, 2015; McGuire et al., 2005; Mountain et al., 2015; Pu et al., 2013; Rodgers, Soulsby, & Waldron, 2005; Rose, 1996; Singh et al., 2016; Soulsby, Malcolm, Helliwell, Ferrier, & Jenkins, 2000) or large (>12,000 km^2) river basins (Brooks et al., 2012; Koeniger, Leibundgut, & Stichler, 2009; Martinelli, Gat, De Camargo, Lara, & Ometto, 2004; Négrel, Petelet-Giraud, & Millot, 2016; Wang et al., 2009), few have simultaneously incorporated a spatially extensive focus with high-sampling frequency on headwater catchments, large tributaries, and mainstem sites at the mesoscale (Jeelani, Saravana Kumar, & Kumar, 2013; Ogrinc, Kanduč, Stichler, & Vreča, 2008; Speed, Tetzlaff, Hrachowitz, & Soulsby, 2011). Many investigations into streamwater source variability conducted within mesoscale basins incorporate only on short duration isotopic sampling (Martinez, Raiber, & Cox, 2015; Séguis et al., 2011; Tetzlaff, Uhlenbrook, Eppert, & Soulsby, 2008) or focus only on major tributaries and river mainstems (Pereira et al., 2014; Rugel, Golladay, Jackson, & Rasmussen, 2016; Scholl et al., 2015). In these complex systems, coupling extensive (in space) with frequent (in time) water sampling during at least an entire year would provide information about regional controls on the spatial and temporal variability of water sources relevant to management.

The water stable isotopes heavy oxygen ($\delta^{18}O$) and deuterium ($\delta^{2}H$) have been extensively used for the determination of fractional contributions to stream water source, and origin of transported water on a wide range of geographic and temporal scales (Brooks et al., 2012; Gibson et al., 2005; Jasechko, Kirchner, Welker, & McDonnell, 2016; Koeniger et al., 2009; Martinelli et al., 2004; Mountain et al., 2015; Schulte et al., 2011; Wang et al., 2009), mean transit times at different time scales (see reviews by McGuire and McDonnell (2006) and Klaus and McDonnell (2013), and flow paths (McGlynn, McDonnel, & Brammer, 2002; Rodgers et al., 2005). Water stable isotopes exhibit systematic spatial and temporal variations resulting from isotope fractionations that accompany water cycle phase changes and diffusion. These properties often impart differing isotopic signatures to rainwater, groundwater, and surface water, allowing for the analysis of hydrologic flow paths and the investigation of component mixing within water bodies. Isotope fractionation is the primary force acting to produce variations in $\delta^{2}H$ and $\delta^{18}O$ values (both spatially and temporally) in water sources across the globe (Araguas-Araguas, Froehlich, & Rozanski, 2000). A prime example of this mechanism is the Rayleigh rainout effect, according to which, progressive isotopic depletion of precipitation is observed as elevation and distance from the original vapor source increase (Araguas-Araguas et al., 2000; Dutton, Wilkinson, Welker, Bowen, & Lohmann, 2005; Wassenaar, Van Wilgenburg, Larson, & Hobson, 2009; Williams & Rodoni, 1997; Yonge, Goldenberg, & Krouse, 1989).

Several previous studies have exemplified the consistent relationship between elevation and surface water stable isotopic concentration at the river basin scale (Bershaw, Saylor, Garzione, Leier, & Sundell, 2016; Biggs et al., 2015; Brooks et al., 2012; Fan, Chen, Li, Li, & Li, 2015; Li et al., 2015; Peng, Chen, Zhan, Lu, & Tong, 2015; Vespasiano et al., 2015; Wassenaar, Athanasopoulos, & Hendry, 2011). For most areas, an elevation lapse rate of ~3‰ km^{-1} for $\delta^{18}O$ can typically be assumed, with the exception of the Himalayas and areas with elevations greater than 5000 m (Poage & Chamberlain, 2001). However, within certain regions that do not meet the high-elevation exception, this correlation has proven to be weak, absent, or even inverse (Bershaw, Penny, & Garzione, 2012; Lechler & Niemi, 2011; Wassenaar et al., 2009). For example, no stable isotope-elevation relationship is observed across the leeward side of the Oregon Coast Range (Brooks et al., 2012). Although the Western Oregon Cascades are impacted by the same storm systems and exhibit a strong correlation between elevation and surface water isotopic composition, surface water isotopes along the leeward side of Oregon Coast Range are unrelated to elevation (Brooks et al., 2012). Additionally, the isotopic signature at the outlets of these leeward watersheds were more enriched than the majority of small catchments within the watershed (Brooks et al., 2012). These observations suggest that local atmospheric or hydrologic mechanisms are effectively overriding the elevation effect within this region, indicating that certain attributes of catchments within the leeward side of the Coastal Range cause them to behave fundamentally differently than those on the windward side of the Cascades.

The objective of our study was to investigate the mechanisms governing seasonal and spatial variations in the isotopic signature of surface waters and their influence upon water supply dynamics and source within the Marys River Basin (MRB, 390.4 km^2) in the leeward Oregon Coast Range. Additionally, we aimed to provide potential explanations for the absence of the stable isotope-elevation

relationship within surface waters in the Coast Range, and to further understand why the isotopic signature within the Marys River was more enriched than local precipitation (Brooks et al., 2012). Understanding the controls on the variability of source water dynamics within the MRB is particularly important because the river serves as the primary source of municipal water for the cities Corvallis and Philomath and provides significant amounts of water to local agricultural operations. Given the increasing prevalence of drought and record low flows such as those observed in the summer of 2015 (www.oregon.gov/owrd/WR/docs/Drought_Information_Statement_Nov_2015.pdf), the need to understand the spatial and temporal variability in the sources of water the MRB is paramount. To accomplish these objectives, we selected 24 sites within the MRB ranging in size from 0.2 km^2 to 390.4 km^2 and monitored surface water isotopic composition every 3 weeks over the course of a year. We then investigated the relationship between tributary and mainstem surface water stable isotopic composition and local isotopic precipitation values collected at six sites in order to identify correlations with surface water isotopic composition. Ultimately, we used the identified correlations to create a two end-member mixing model, which informs our understanding of seasonal spatial sources of water dynamics within the basin.

2 | METHODS

2.1 | Study site

The Marys River, located in Oregon's Western Coastal Range, is an 80 km long 5th order stream with a drainage area of 390.4 km^2 (Figure 1). The river has an average annual discharge of over 400 million m^3/year and serves as the primary source of municipal water to the city of Corvallis, OR (USGS gauge number 14171000). Elevation within the basin ranges from 70 m at the valley floor to nearly 1,300 m at Marys Peak. The basin is characterized by a Mediterranean climate with warm, dry summers and mild, wet winters. Mean annual precipitation ranges from 1,000 mm at the lower elevations to greater than 2,500 mm at the high elevations, with a rain-dominate regime at elevations below 400 m and a snow-dominate regime above 1,200 m (Jefferson, 2011; Leibowitz, Wigington, Comeleo, & Ebersole, 2012; Mattson et al., 1999). For the purpose of our study, 24 subbasins, which represent a number of small to large tributaries and mainstem sites, were selected within the MRB (Figure 1). These catchments range in size from 0.23 km^2 to 390.4 km^2 (mean = 71.6 km^2) and occupy elevations from 62 m to 636 m.a.s.l (mean = 174 m.a.s.l.). We used the USGS gauge to delineate our study watershed boundaries.

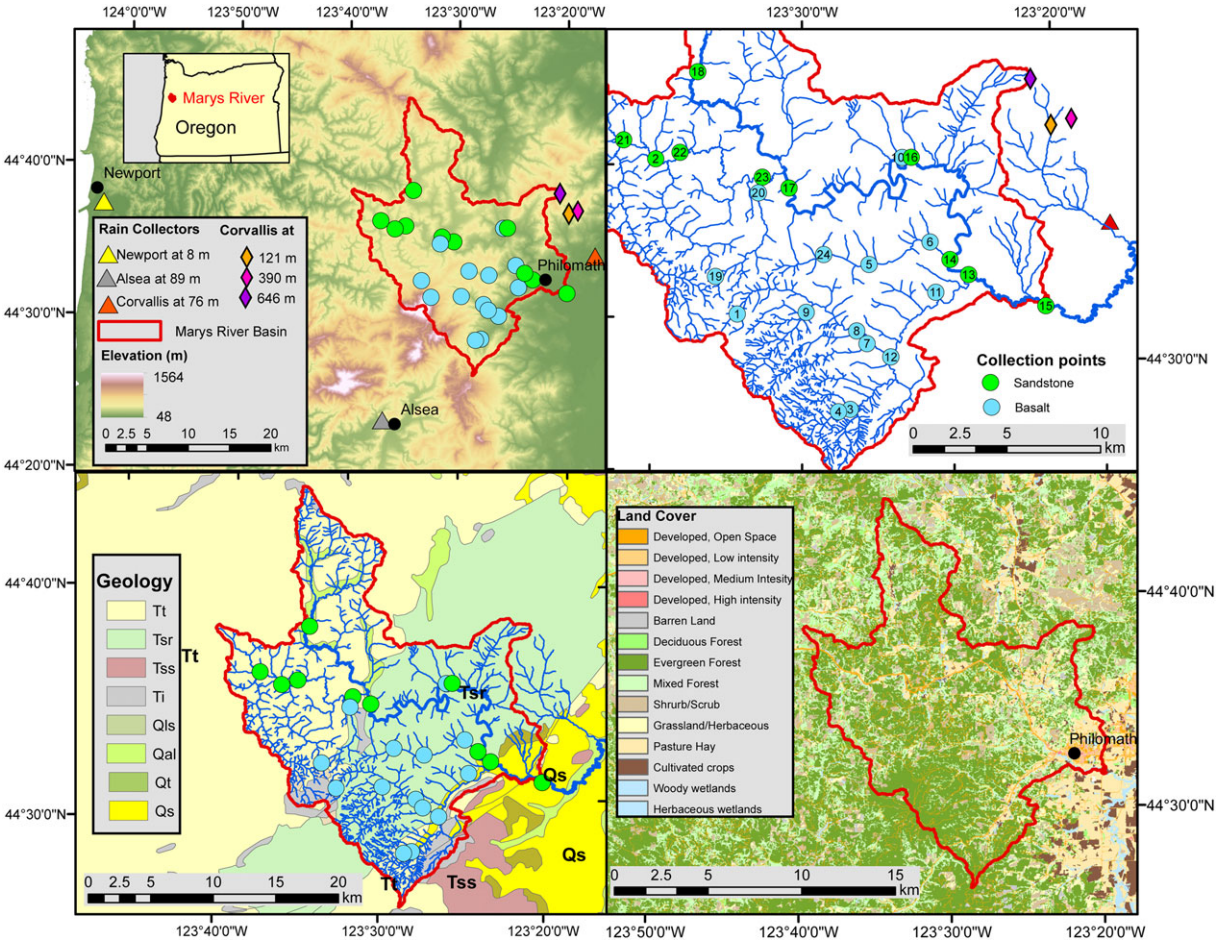

FIGURE 1 Location of the Marys River Basin, grab water sampling locations (n = 24), and precipitation collection sites in Corvallis (n = 4), Alsea, and Newport. Predominate geology types of the Marys River Basin including basalt (Ti & Tsr), sandstone/siltstone (Tss & Tt), and quaternary sediment (Qal, Qls, Qs, & Qt) (Walker & MacLeod, 2002), and land cover in the basin (Homer et al., 2015)

The geology of the MRB is characterized primarily by a mixture of sedimentary formations (marine sediment), volcanic and intrusive rocks, and sparse quaternary sediment (alluvium and colluvium) (Baldwin, 1964; Walker & MacLeod, 2002). Geologic composition within the MRB is dominated by basalt (Figure 1: Ti & Tsr) and sandstone/siltstone (Figure 1: Tss & Tt), with few areas underline by quaternary deposits (Figure 1: Qal, Qls, Qs, & Qt,) with these rock types occupying 49, 41, and 9% of the total drainage area, respectively. The north, west, and southwest boundaries of the watershed are formed by sloping to very steep uplands composed of volcanic, sedimentary, and intrusive rocks of the northern Coast Range (Baldwin, 1964; O'Connor et al., 2014; Rhea, 1993; Walker & MacLeod, 2002). Quaternary sedimentary deposits occupy the small sections in the southeast portion of the basin and are comprised of Holocene to Pleistocene landslides, sand, gravel, clay, mud/silt, and gravel/terrace deposits. Basaltic lava flows and intrusive deposits underlie the central and northeast portions of the basin and consist of Oligocene gabbros and Paleocene to Middle Eocene tholeites (Walker & MacLeod, 2002). Middle Eocene to Late Eocene deposits of mudstone, sandstone, and siltstone underlie much of the northwestern and southeastern portions of the basin (Figure 1).

According to the National Land Cover data base (Homer et al., 2015), land cover within the MRB is highly variable but can be typified into three primary categories: forest, agriculture, and urban development (Figure 1). Total land cover is dominated by vegetation (68.1%), with the largest categories being evergreen forest (32.5%), shrub/scrub (14.1%), and mixed forest (11.6%). Crop cultivation, hay, and pasture fields comprise 22.0% of the total land area. High, medium, and low intensity development areas within unincorporated communities, towns, and cities occupy approximately 10% of the basin. The highest concentration of development is located near the confluence of the Marys and Willamette River and associated with the cities of Philomath and Corvallis, with total populations of 4,584 and 54,462, respectively (U.S. Census Bureau, 2015).

2.2 | Field methods

Twenty-four sites were selected for surface water sample collection on a 2–3 week basis from November 2014 to September 2015 for 12 sampling events and 279 samples. Twenty-two samples were not collected due to access restrictions associated to road closures during winter conditions and logging operations. The selected sites included 15 tributary and mainstem sites sampled for surface water isotopes by Brooks et al. (2012) that were selected to cover the range of catchment elevations within the watershed. An additional nine sites were chosen to enhance spatial coverage of smaller tributaries and headwater catchments within the MRB in order to interpret isotopic variation on a finer scale. Precipitation collectors were constructed following IAEA protocols (Groning et al., 2012) to prevent evaporation and installed at four sites (Figure 1) across a range of elevations (76, 121, 390, and 646 m.a.s.l., respectively). The precipitation samplers were located outside the study basin (5–12 km from gauged outlet) but still within the full MRB. We were not able to collect precipitation samples inside the study basin given access restrictions. Precipitation samples at three higher elevation sites were collected on a monthly basis from October of 2014 through September of 2015. Isotopic precipitation data were collected on a weekly basis from June of 2014 to June of 2015 in the lower elevation site in Corvallis (76 m.a.s.l) and from January of 2014 to December of 2015 in Newport (8 m.a.s.l), near the Coast on the west side of the Coast Range (Figure 1). These weekly data were supplied by the U.S. Environmental Protection Agency Western Ecology Division. Precipitation data collected in Alsea (89 m.a.s.l, located in the central Coast Range) (Figure 1) from 1989 to 2006 on a monthly or bimonthly basis was supplied by the U.S. Network for Isotopes in Precipitation. Surface water and precipitation samples were sealed in 20 mL screw top glass vials with conical inserts and capped without headspace in order to prevent isotopic fractionation. Duplicates were collected every 10 samples for quality assurance and control. Prior to analysis, all samples were stored upside down in a dark, temperature-controlled environment.

2.3 | Isotopic and statistical analysis

Water isotope analysis was performed using a cavity ring down spectroscopy liquid and vapor isotopic measurement analyzer (Picarro L2130-*i*, Picarro Inc, CA). The L2130-*i* is a time-based measurement system that uses a laser to quantify spectral features of gas phase molecules (specifically absorption lines unique to $H_2{}^{16}O$, $H_2{}^{18}O$, and $HD^{16}O$) in an optical cavity (Picarro 2010). Samples were run under high-precision analysis mode using a 10 µL syringe for six injections per sample, with the first three injections discarded to eliminate memory effects. The internal standards used to calibrate each run included MET-1 ($\delta^{18}O$ = −14.49‰, $\delta^{2}H$ = −107.21‰) and BB-1 ($\delta^{18}O$ = −7.61‰, $\delta^{2}H$ = −50.72‰). The internal standard ALASKA-1 ($\delta^{18}O$ = −11.09‰, $\delta^{2}H$ = −78.8‰) was used to calculate accuracy and duplicate field samples were used to assess precision. All internal lab standards were originally calibrated to the IAEA primary standards for Vienna Standard Mean Ocean Water ($\delta^{18}O$ = 0.0‰, $\delta^{2}H$ = 0.0‰), Standard Light Antarctic Precipitation ($\delta^{18}O$ = −55.5‰, $\delta^{2}H$ = −427.5‰), and Greenland Ice Sheet Precipitation ($\delta^{18}O$ = −24.76‰, $\delta^{2}H$ = −189.5‰). Isotopic values were reported as delta (δ) values and presented in parts per thousand (‰) deviation from the adopted standard representing mean isotopic composition of the global ocean (Vienna Standard Mean Ocean Water):

$$\delta = \left(\frac{R_{sample}}{R_{standard}} - 1\right), \qquad \text{(Equation 1)}$$

where R_{sample} and $R_{standard}$ are the isotope ratio ($\delta^{2}H$ /H or $^{18}O/^{16}O$) in the samples and standard, respectively (Craig, 1961). Measurement precision was determined with the use of internal standards and duplicate samples and was 0.05‰ and 0.21‰ for $\delta^{18}O$ and $\delta^{2}H$, respectively.

All statistical analyses were conducted using the MATLAB Statistics and Machine Learning Toolbox. All data sets of $\delta^{18}O$, $\delta^{2}H$, and deuterium excess in precipitation and surface samples were tested for normality. Differences across normally distributed data were tested using parametric test including *t* student (*t* test), analysis of variance, and Tukey test whereas differences across nonnormally distributed

data were performed with nonparametric statistics such as Mann–Whitney U test (M-W).

2.4 | Global and local meteoric water lines

In order to assess regional trends and to verify that surface water samples had not undergone fractionation a regional Local Meteoric Water Line (LMWL) for the Coast Range was established based on the precipitation water stable isotope data from Newport, Corvallis, and Alsea, OR, and compared to the Global Meteoric Water Line ($\delta^2H = 8 \times \delta^{18}O + 10$, GMWL). LMWLs were also constructed for each geographic site independently in order to assess local climatic variations on the windward (Newport), central (Alsea), and leeward (Corvallis) regions of the Coast Range.

Deuterium excess (d-excess) values were calculated for all precipitation and surface water samples collected over the duration of the study in order to assess seasonal trends and discard samples that were heavily influenced by evaporation. The d-excess parameter is defined by $d\text{-}excess = \delta^2H - 8\delta^{18}O$ (Dansgaard, 1964).

2.5 | End-member mixing analysis

A simplified two end-member mixing model was used in order to estimate temporal variations in the contributions from sandstone- and basalt-based catchments to Marys River. For the application of this model, it is assumed that basalt and sandstone contributing areas make up the entirety of discharge contributed to the stream and exiting at the outlet. The model is composed of two equations:

$$F_{ss}\left(\delta^{18}O_{ss}\right) + F_b\left(\delta^{18}O_b\right) = \delta^{18}O_{outlet}, \quad \text{(Equation 2)}$$

$$F_{ss} + F_b = 1, \quad \text{(Equation 3)}$$

where F_{ss} (fraction from sandstone catchments) multiplied by the average $\delta^{18}O$ value of sandstone catchments plus F_b (fraction from basalt catchments) multiplied by the average $\delta^{18}O$ value of basalt-based catchments yields the $\delta^{18}O$ value of stream water at the watershed outlet, and both fractions add to one. The calculations were then repeated with δ^2H substituted in place of $\delta^{18}O$. An average value for the fractional contributions from basalt and sandstone catchments was then computed from the results of the two models.

3 | RESULTS

3.1 | Local meteoric water line and precipitation water stable isotopes

Precipitation water stable isotopes in Newport (8 m.a.s.l., 2008–2015), Alsea (89 m.a.s.l, 1989–2006), and Corvallis (76 m.a.s.l., 2002–2015) decreased moving inland, with precipitation amount weighted means of −7.0, −8.5, and −9.1 for $\delta^{18}O$ and −46.7, −58.2 and −63.5 for δ^2H, respectively. A distance from the ocean lapse rate of −3.5‰ per 100 km for $\delta^{18}O$ and −27.5‰ per 100 km for δ^2H ($R^2 > 0.95$, $p < .015$) was calculated from the coast (Newport) to the leeward side of the Coast Range (Corvallis). LMWLs constructed for each location indicated no statistically significant local differences (analysis of variance f-stat = 0.13, $p = .88$). The regional LMWL generated from precipitation collected all three sites (Alsea, Newport, and Corvallis) yielded a line with a slope of 7.8 and intercept of 7.4, which was not significantly different (*t* test, $p < .01$) from the GMWL. The regional LMWL demonstrated agreement with previous LMWL calculations ($\delta^2H = 7.6 \times \delta^{18}O + 6.1$ for precipitation in Corvallis, (Brooks et al., 2012).

Precipitation-weighted means of weekly precipitation isotopes in Corvallis (76 m.a.s.l.) collected during the study period (June 2014 and October 2015, $n = 39$) were isotopically heavier than the long-term average with precipitation weighted means of −58.8 and −8.5 for δ^2H and $\delta^{18}O$, respectively, for the study period compared to −63.8 and −9.0 for δ^2H and $\delta^{18}O$ for the long-term average. Weekly precipitation isotope values within this period varied from −3.5 to −12.7 for $\delta^{18}O$ and −22.1 to −93.6 for δ^2H (Figure 2). d-excess values ranged from −0.5 to 18.9‰, with a volume weighted average value of 9.2‰ ± 3.9. Ten samples (25%) fell 5‰ or more below the GMWL indicating evaporation (Brooks et al., 2012). Of these 10 samples, 70% were collected during the spring and summer months when storm magnitude is at a minimum and evaporative influences are likely to be strongest.

No statistically significant seasonal differences were detected in $\delta^{18}O$ or δ^2H of precipitation in Corvallis (76 m elevation) during the study period (Figure 2). Mean summer precipitation values were characterized by the lowest values of d-excess (2.9‰ ± 1.7‰), indicating the greatest deviation from the GMWL (Figure 2).

We found that mean magnitude-weighted precipitation isotopic signatures decreased with increasing elevation (Figure 3). Isotopic signatures of precipitation were the most enriched in the valley bottom at 76 m ($\delta^{18}O$ = −8.6‰ & δ^2H = −59.1‰) and were more depleted as they approached the highest measured elevation at 646 m ($\delta^{18}O$ = −9.9‰ & δ^2H = −67.1‰). The elevation lapse rate indicated a decrease in $\delta^{18}O$ and δ^2H values by 2.1‰ km^{-1} and 12.5 ‰ $km^{-1}$of elevation gain (R^2 = 0.83–0.89, $p = .05$–.09), respectively (Figure 3).

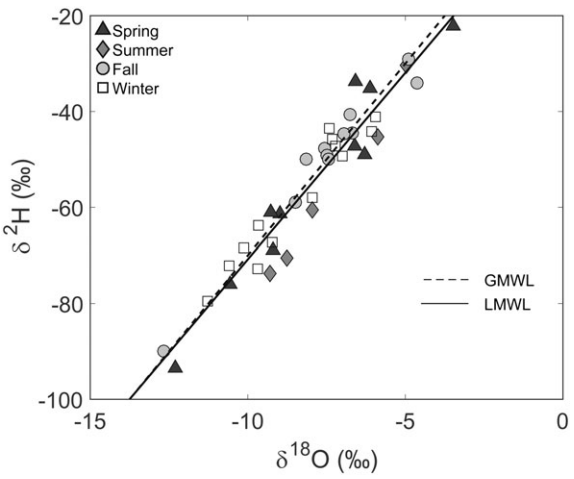

FIGURE 2 Isotopic precipitation values in Corvallis at 76 m (Figure 1) by season between June 2014 and October 2015; the LMWL was derived based on 39 samples. GMWL = Global Meteoric Water Line; LMWL = Local Meteoric Water Line

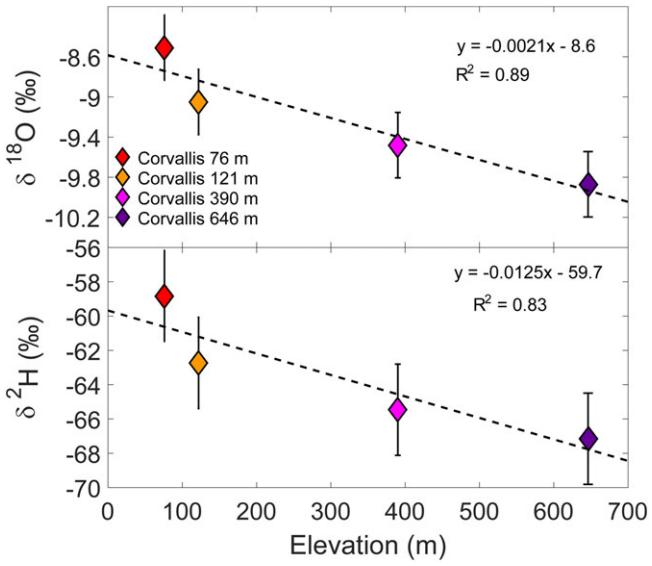

FIGURE 3 Relationship between annual (2014–2015) average volume weighed $\delta^{18}O$ (‰) and $\delta^{2}H$ (‰) of precipitation and elevation at the Corvallis collection sites (see Figure 1 for location). The error bars represent the precipitation-weighted standard errors

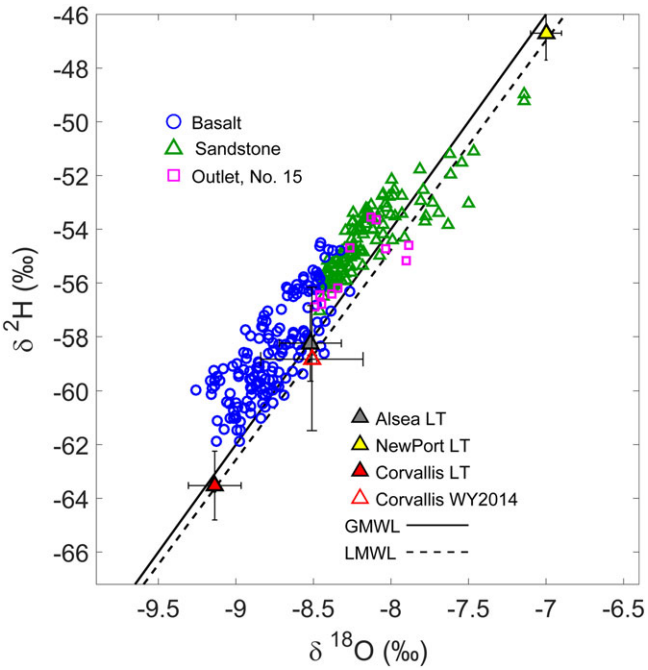

FIGURE 4 Variation in surface water and precipitation isotopes. Blue circles and green triangles represent 3-week (n = 279) surface water stable isotope values for the 24 selected catchments over the duration of the study (Figure 1). Samples collected at the outlet (site no. 15, Figure 1) are pink squares. The lines represent the global and local meteoric water lines (GMWL solid line and LMWL dashed line, respectively). Solid triangles are long-term isotope precipitation mean volume-weighted values for Newport (8 m.a.s.l., 2008–2015), Alsea (89 m.a.s.l., 1989–2006), and Corvallis (76 m.a.s.l., 2003–2015). Mean volume weighted precipitation values for Corvallis during the collection period (June 2014–September 2015) is also indicated (hollow red triangle). GMWL = Global Meteoric Water Line; LMWL = Local Meteoric Water Line

3.2 | Temporal and spatial variation of surface water isotopes

Surface water isotopes within the MRB ranged from −9.3 to −7.1‰ in $\delta^{18}O$ and from −61.9 to −49.0‰ in $\delta^{2}H$ (Figure 4). All surface water samples fell on or slightly above the GMWL indicating no evaporative influence (Figure 4). d-excess values ranged from 6.9 to 14.1‰ with an average value of 11.3‰ ± 0.07‰. We found two distinctly separate groups of catchments that helped explain the variation in surface water isotopes: the first group (n = 10) was characterized by isotopically enriched values (isotopic signatures vary between −8.49‰ & −7.14‰ and −57.06‰ & −48.99‰ for $\delta^{18}O$ and $\delta^{2}H$, respectively, green triangles, Figures 4 and 5), and the second group (n = 14) was characterized by isotopically depleted values (isotopic signatures vary between −9.26‰ & −8.27‰ and −61.87‰ & −54.52‰ for $\delta^{18}O$ and $\delta^{2}H$, respectively, blue circles, Figure 4 and 5). The predominate underlying geology of the catchments correlated strongly with the two identified groups (Figures 1, 4, and 5). Group 1 contained nine catchments (90%) primarily drained by sandstone (52–100% in area) with the exception of the outlet (USGS gauge, site no. 15, Figure 1) in which sandstone was 41% of the catchment. Group 2 contained catchments primarily drained by basalt (69–100% in area) with the exception of two sites (sites no. 4 and 19) in which basalt covers 40 and 0% of the area, respectively. Mean isotopic values for the complete period of record were significantly different (M-W test, p < .0001) between Group 1 ($\delta^{18}O$ = −8.2‰, $\delta^{2}H$ = −54.4‰) and Group 2 ($\delta^{18}O$ = −8.8‰, $\delta^{2}H$ = −58.6‰). Variability (i.e., standard deviation, SD) among the sandstone sites was highest during fall ($SD_{\delta 18O}$ = 0.3‰, $SD_{\delta 2H}$ = 1.6‰) and lowest during spring ($SD_{\delta 18O}$ = 0.1‰, $SD_{\delta 2H}$ = 1.1‰) (Figure 5). The sandstone sites in Group 1 were located along the main stem of the Marys River and in the northwestern portion of the basin (Figure 1, sites no. 2, 13–18, 21–23). Basalt sites demonstrated a similar pattern with the highest variability in the fall ($SD_{\delta 18O}$ = 0.3‰, $SD_{\delta 2H}$ = 2.1‰) and lowest variability in the spring($SD_{\delta 18O}$ = 0.2‰, $SD_{\delta 2H}$ = 1.4‰). The basalt sites in Group 2 were composed of collection sites located in the central-western and northeastern portions of the MRB (Figure 1, sites no. 1, 3–12, 19, 20, 24).

Sites along the mainstem (no. 10, 13–18) of the Marys River were most isotopically enriched during the summer ($\delta^{18}O$ = −8.07 ± 0.09 ‰, $\delta^{2}H$ = −55.1 ± 0.6‰), while the most depleted values were observed in spring ($\delta^{18}O$ = −8.4‰ ± 0.03, $\delta^{2}H$ = −60 ± 0.3‰). In all seasons, the outlet of the Marys River (Figure 1, site no. 15) underlain similarly by sandstone and basalt deposits (49 and 41% of its area, respectively) reflected a more isotopically enriched signature than most of its tributaries, with similar values to that in Group 1 dominated by sandstone lithology (Figure 4).

Variation in precipitation samples collected across all four collectors did not account for the variation we found across all surface water isotopes within the Marys River during the study period. The average d-excess value for surface water (11.3‰ ± 0.07‰) was significantly higher (M-W U test, p < .0001) than that of precipitation (9.2‰ ± 3.9). Similar to previous analysis of surface water in the Coast Range (Brooks et al., 2012), the isotopic values of surface water showed no systematic depletion with elevation. The slope of the relation between elevation and isotopic concentrations in surface water (−0.0001) was not statistically different from zero (p = .74). Thus, the relationship between increasing elevation and isotopic depletion

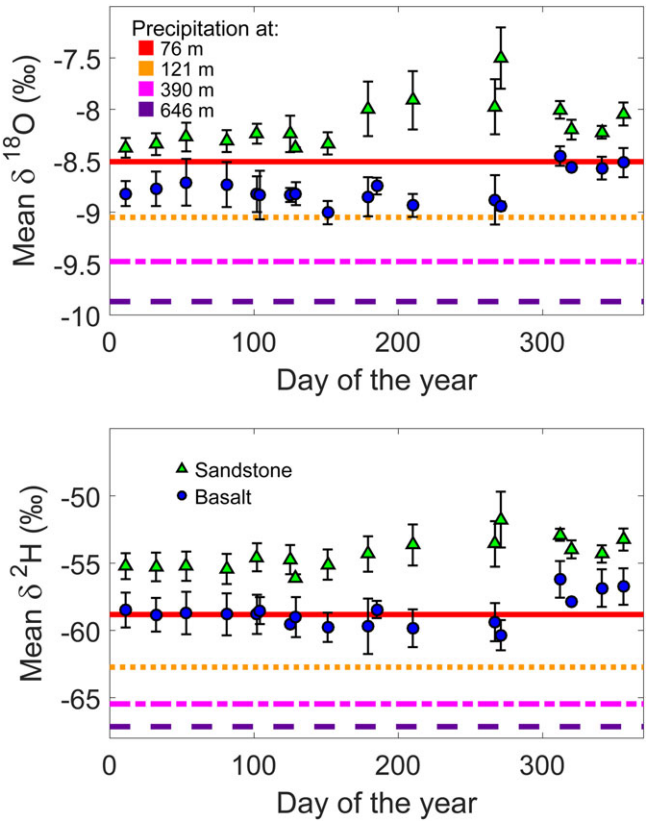

FIGURE 5 Mean $\delta^{18}O$ and δD values for sandstone and basalt catchments during 2014–2015 across all 24 sampling locations (Figure 1). The lines represent annual average volume weighted isotopic precipitation within the Marys River Basin at 76, 121, 390, and 646 m.a.s.l. during the same period (see Figure 1 for sampling locations). The error bars represent standard deviations across all samples collected in a given date

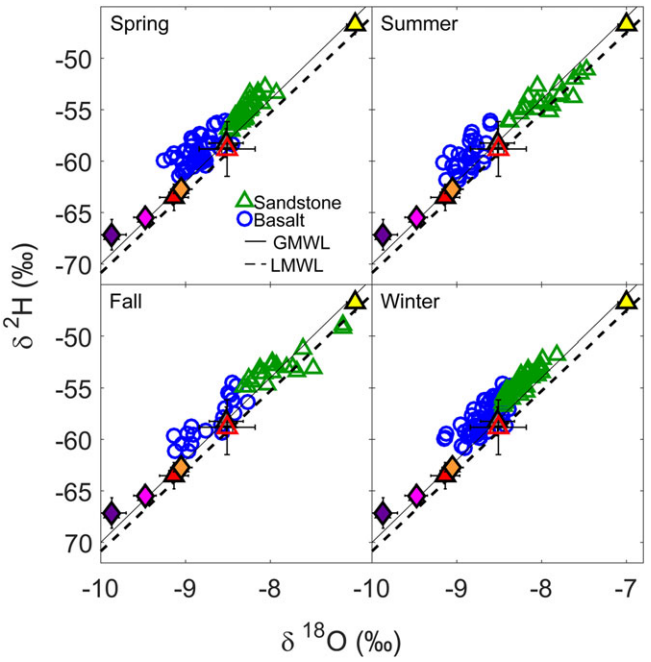

FIGURE 6 Seasonal values of surface water in sandstone and basalt catchments, long-term volume weighted average isotopic precipitation values for Newport (yellow triangle), Alsea (gray triangle), and Corvallis (red triangle) and volume weighted average (2014–2015) isotopic precipitation values in Corvallis at 76 m (open red triangle), 121 m (orange diamond), 390 m (magenta diamond), and 646 m (purple diamond). GMWL = Global Meteoric Water Line; LMWL = Local Meteoric Water Line

observed in precipitation (Figure 3) was not evident in surface water. The mean isotopic signature of precipitation measured at three of the four different elevations was consistently more depleted than the isotopic concentrations from surface water (Figures 4–6). Indeed, a significant difference (*t* test, $p < .001$) existed between mean annual isotopic values of precipitation at three of the four collection sites (at 121, 390, and 649 m.a.s.l) and surface water in sandstone catchments, and between the upper two precipitation collection sites and surface water in basalt catchments ($p < .0002$, Figures 5 and 6). Only precipitation isotope values measured on the windward side of the Coast Range in Newport are more enriched than surface water isotopes measured in the sandstone sites (Figures 4 and 6). Precipitation isotopes measured on the windward side in Alsea had values between the two lithology groups (Figures 4 and 6).

4 | DISCUSSION

4.1 | Trends in precipitation water stable isotopic concentrations

The regional LMWL constructed using isotopic data from the six collection sites indicates that regional isotopic signatures did not deviate significantly from the GMWL. LMWLs specific to Newport, Alsea, and Corvallis shared similar slopes and intercepts to the GMWL, indicating that precipitation within this region was not subject to secondary evaporation. However, precipitation collected during the spring and summer showed the greatest amount of deviation from the GMWL (Figure 2). Due to the careful nature of precipitation collection and the use of evaporation free samplers, samples did not experience evaporation prior to retrieval. Instead, frontal systems during the spring and summer were likely more strongly influenced by nonequilibrium evaporation at the source due to frequent high temperatures during relatively smaller storm magnitudes (Benjamin, Knobel, Hall, Cecil, & Green, 2005; Jeelani et al., 2013).

Spatial trends in the average isotopic values of precipitation across the six collection sites demonstrated notable decreases in isotopic concentration both with distance from the initial vapor source and with elevation. Newport, which represents the windward side of the Coast Range, was characterized by the most isotopically enriched precipitation values (Figures 4 and 6). Isotopic values of precipitation collected in Alsea (middle Coast Range) and Corvallis (leeward Coast Range) demonstrated a continual trend in increasing isotopic depletion as systems move inland. This is consistent with observations in Western and Coastal Southwestern Canadian surface water (Yonge et al., 1989). The calculated precipitation elevation lapse rate for the leeward side of the Coast Range (2.1‰ km^{-1} for $\delta^{18}O$ and 12.5‰ km^{-1} for $\delta^{2}H$) were 25–39% smaller than lapse rate calculations (2.8‰ km^{-1} for $\delta^{18}O$ and 20.6 ‰ km^{-1} for $\delta^{2}H$) previously performed for surface water in the Willamette River Basin (Brooks et al., 2012). This indicated an overall slower rate of depletion in the leeward side compare to the

windward side of the Cascades Mountains. However, our values represent a higher rate of depletion (30–20%) than the lapse rates calculated for high-elevation springs in the Cascade mountains, which spanned the windward to leeward sides of those mountains (1.6‰ km^{-1} for $\delta^{18}O$ and 10.57 ‰ km^{-1}; Jefferson, Grant, & Rose, 2006). Thus, our lapse rates fall somewhere in between those other local lapse rates. Given that our analysis only included precipitation samples collected over 1 year, the calculated lapse rates could also be a reflection of specific conditions during 2014–2015. Despite the similarity between our precipitation lapse rates and those within surface samples in the Willamette and the Coastal and Western Canadian ranges, our results also confirmed the lack of elevation-isotope concentration relation in surface water on the leeward side of the Oregon Coast Range.

Given that a strong relationship between mean watershed elevation and surface water isotopic values has been exemplified in the Cascade Range, one potential explanation for the lack of this relationship in the Coast Range might arise from differences in local atmospheric dynamics occurring on the leeward side of the range. However, since we found an elevation relationship with precipitation, and the LMWL's were similar to the GMWL, variations in atmospheric conditions does not seem a plausible explanation for the lack of an elevation influence on surface water isotopes. One complication is that our precipitation collectors for our elevation pattern were all located just outside our study basin, in the eastern portion of the MRB, and thus may not reflect the full variation in precipitation isotopes across the MRB. The range of precipitation isotopic concentrations within the MRB likely falls between the concentrations registered in the Alsea watershed (Figures 4 and 6, southwest of MRB and on the windward side of the Coast Range) and those registered in our four sampling locations East of the basin (Figure 1). This range of precipitation isotope values would explain our highest elevation site (site 1, 731 m.a.s.l. with basalt geology), which were more enriched than expected given our elevation pattern. Using the equations in Figure 3, we would predict precipitation isotope values at that elevation to be −10.1‰ and −68.8 ‰ for $\delta^{18}O$ and $\delta^{2}H$, respectively; however, surface water isotopes for this site averaged −8.9‰ and −58.2‰, which is more similar to the precipitation isotope values at the Alsea site (−8.5‰ and −58.2‰). Most of basalt-dominated catchments have surface water isotope values that are bracketed by these two precipitation endmembers (Figure 4). However, the isotopic concentration measured in sandstone-dominated surface water catchments within the basin fell well above this range, falling between precipitation isotopes measured at Alsea and Newport that represent the windward side of the Coast Range (Figures 4 and 6, green triangles). Alternatively, to precipitation driven processes, surface or subsurface-based hydrologic properties could be responsible for the dampening of the rainout effect in surface water isotopic signatures. Indeed, for the entire Marys Basin, our data suggest that geological properties are also playing a large role in the spatial variation of surface water isotope values.

4.2 | Spatial and temporal trends in surface water isotopic composition

Similarly to results in a mesoscale (749 km^2) Scottish watershed (Capell, Tetzlaff, Hartley, & Soulsby, 2012), we found that the spatial variations and temporal trends in surface water stable isotope values reflected variability in underlying catchment geology. This might be an expression of the controlling effects of rock permeability on hydrological conditions reported in small catchments. For instance, soil depth and hydraulic connectivity were highly influential on water isotope values in small (<1 km^2) arid systems (Heidbuechel, Troch, & Lyon, 2013); topographic organization was another factor influencing water isotope values in humid 3–5 km^2 temperature catchments (Singh et al., 2016); and storage had a large effect on water isotope values on humid 3.2 km^2 systems (Blumstock et al., 2015; Soulsby et al., 2015). In the MRB, the degree of difference between isotopic values within basalt- and sandstone-based catchments was smaller during the winter and spring when precipitation was high and higher during the summer and fall when precipitation amounts were much lower (Figure 5). with sandstone catchments always having more isotopically enriched surface waters. During the drier months when streams were at baseflow conditions, the two groups demonstrate a very dramatic separation, indicating that baseflow was being supplied from two isotopically distinct water sources: one isotopically more similar to precipitation within the Marys Basin that supplied basalt catchments, and the other isotopically more enriched that the measured precipitation sources in the basin that supplied sandstone catchments. We speculate that sandstone formations crossing the Coast Range divide to the East may facilitate cross-basin water exchange of groundwater. Even though the overall sandstone dipping appears to be West (Wiley, 2008), cross-basin water exchange, could be occurring at local dipping or fracture sandstone facies (Hale & McDonnell, 2016) or through fractured underlying basalt or intrusives (Figure 1). In any case, these geologic features would be capable of transmitting more isotopically enriched precipitation falling on the windward side of the Coast Range, resulting in more enriched surface water and groundwater isotopic values within sandstone drained catchments in the Marys Basin. Although from a different sandstone facies, Hale et al. (2016) reported isotopic values of groundwater measured in highly and deeply fractured sandstone in the windward side of Coast Range of −50 ‰ for $\delta^{2}H$, which matches our sandstone eastern most surface water isotopic values during the summer low flow (site no. 18, Figure 1). Alternative explanations such as variable recharge or isotopic alteration of groundwater are not likely. Variable isotopic composition during periods of active recharge could not account for the geological differences given the close proximity of the selected catchments and relatively consistent nature of storm duration, magnitude, and areal storm extent over the basin. Although rates of recharge may vary depending on local permeability and saturation, the isotopic composition of the infiltrated precipitation should be fairly uniform. In addition, the spatial variation in precipitation isotope values in the Marys Basin were all more depleted than surface water isotope values coming from sandstone (Figures 4 and 6). Chemical fractionation is also unlikely despite the similarities between the kaolinite reaction line and the GMWL (Sheppard & Gilg, 1996) because of the conservative nature of water stable isotopes. Unlike isotopes of carbon and sulfur, concentrations of $\delta^{18}O$ and δD are not substantially altered during reactions with minerals along shallow, low-temperature flow paths (Kendall & McDonnell, 1998).

For both geological catchment types, the isotopic composition of surface water within the MRB exhibited only a fraction of the seasonal variation that we found in precipitation, suggesting that the fraction of precipitation routed directly to the stream as event water is typically not the dominate factor influencing the isotopic composition of surface water. Consequently, stored water (e.g., groundwater or pre-event water) was likely the strongest driver of the differences observed in surface water. For both geological groups, the average d-excess value for surface water was significantly higher than that of precipitation. Given that evaporation produces lower d-excess values and shifts points below the GMWL, evaporation was not the primary driver of this difference. Instead, we suspect that the isotopic value of precipitation that contributes to groundwater recharge (which may be stored in hillslopes, bedrock, or riparian areas) must be isotopically different from the average annual precipitation value within the Marys Basin. For simplicity sake, we will focus on surface water within the basalt catchments, which we speculate originated in a higher proportion from precipitation within the Marys Basin. The discrepancy between the isotopic signature of recharge (i.e., groundwater) and average annual precipitation is likely due to seasonal variations in recharge capacity as a result of antecedent soil moisture and storm intensity, with large fall and winter storms having higher d-excess values. This theory is further supported by the significant difference between mean annual isotopic values of precipitation and surface water in sandstone catchments and mean weighted isotopic concentrations of precipitation at three different elevations (Figures 4 and 6). The largest disparity between isotopic values of precipitation and surface water is present in the fall, whereas greatest degree of similarity exists in winter. During early fall, streams are generally at or near baseflow conditions due to the absence of significant rainfall throughout the summer, typical of maritime climate. As a result, surface water isotopic signatures at this time are the most strongly representative of groundwater sources (Freeze, 1974). Conversely, during the peak of the winter rainy season streams are at their highest flow levels due to large-magnitude and long-duration storms. Thus, it is not surprising that surface water was most isotopically consistent with precipitation during the wettest portion of the year when the fraction of precipitation as streamflow is highest and most isotopically dissimilar when conditions were driest.

Because the two geological catchment groups have such distinct isotopic signatures for surface water, we estimated their fractional contributions to streamflow at the outlet over the study period (Figure 7). Using a simple mixing model, we estimated that the sandstone catchments contribute on average 77% of the flow annually compared to 23% from basalt catchments. The contribution from basalt were highest during the wet period (January–April; Figure 7b). This suggests that water storage within the basalt is comparatively "flashier" than that of sandstone, meaning that during wet conditions water is quickly routed off of the low-permeability basalt bedrock. Due to lower permeability, storage within the basalt is more rapidly depleted during dry periods absent of recharge. Similarly, more isotopically depleted values were reported in watersheds underline by crystalline versus sedimentary lithology (Capell et al., 2012). In our case given that basalt underlies 49% percent of the basin, this holds significant implications for streamflow within catchments during low-flow periods and drought years. These basalt catchments in the central portion of the basin may be subject to a substantial decline in streamflow yet make up the majority of the Rock Creek watershed supplying water to the city of Corvallis. During the dry summer period, the higher permeability sandstone-drained catchments to become the primary contributors to streamflow, contributing over 80% of the flow during these critical low-flow periods. Sandstone catchments along the western side of the basin may be continuously fed by highly fractured, cross-basin sandstone aquifers during these periods, essentially providing a subsidy of water to the Marys River besides local precipitation.

Our results provide strong evidence of significant cross-basin water exchange and challenge topographic derived watershed boundaries. As previous studies have highlighted, topography is not the sole attributes controlling spatiotemporal patterns in streamflow (Brooks et al., 2012; Klaus & McDonnell, 2013; McGuire et al., 2005; Mountain et al., 2015). In fact, many studies have highlighted shortcomings of topography as the primary control, and other factors such as soil thickness and moisture (Buttle, Dillon, & Eerkes, 2004; Devito et al., 2005; Grayson & Western, 2001), distribution of flow paths and runoff

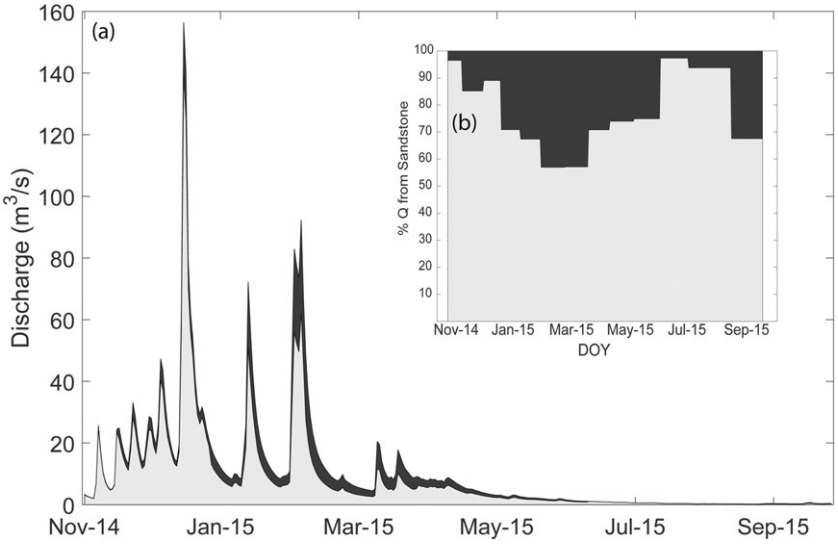

FIGURE 7 (a) Hydrograph of total discharge and basalt and sandstone drained catchment contributions at the catchment outlet point (site no. 15, Figure 1) derived from mixing model results of $\delta^{18}O$ and $\delta^{2}H$ (Equations 2 and 3); (b) Time series of fractional contributions from sandstone and basalt

responses (Buttle, Creed, & Moore, 2005; McDonnell, 2003), wetness indices (Grabs, Seibert, Bishop, & Laudon, 2009), water tables (Condon & Maxwell, 2015; Haitjema & Mitchell-Bruker, 2005; Moore & Thompson, 1996), and ground water residence times (Maxwell et al., 2016; McDonnell et al., 2010). Nevertheless, topographic boundaries continue to be the most common approach to delineating watersheds. Our study clearly indicates that topography is likely insufficient to define watershed boundaries in permeable sedimentary rocks; highlighting the overwhelming importance of underlying geology.

5 | CONCLUSIONS

Combined analysis of precipitation and surface water isotopic composition was highly valuable in identifying correlations between catchment geology and isotopic composition and interpreting seasonal variations in the source of water contribution to the MRB. Our findings challenge the topographic derive watershed boundaries and suggest that geologic controls on hydrologic flow paths and cross-basin water exchange serve as likely explanations for the lack of relationship between surface stable isotope and elevation within the Coast Range of Oregon. This results are likely relevant to other watershed underlie by permeable material. Additionally, our results reaffirm that hydrologic behavior within the western Willamette River Basin along the leeward side of the Coast Range cannot be assumed to reflect the same seasonal and spatial variations that might be observed along the eastern side of the valley within the Cascade Range.

Furthermore, these findings hold significant implications for water supply to the cities of Corvallis and Philomath, given that Marys River serves as one of the primary sources (over 30%) of municipal water to these locales. Because basalt dominated catchments are prone to greater flashiness and make up a lesser amount of overall streamflow during dry periods, prolonged drought has the potential to lead to water shortages for the surrounding areas. Ultimately, the methodology applied here could be replicated to determine controlling factors of surface water isotopic composition within other areas where the stable isotope-elevation relationship is absent and where permeable material is likely to favor cross-basin water exchange.

ACKNOWLEDGMENTS

This work was funded in part by the H.J. Andrews Experimental Forest LTER7 (NSF Award #1440409), the USDA National Institute of Food and Agriculture; McIntire Stennis project OREZ-FERM-876 and the Department of Forestry Engineering Resources and Management at Oregon State University (OSU). This manuscript has been subjected to Agency review and has been approved for publication. The views expressed in this paper are those of the author(s) and do not necessarily reflect the views or policies of the U.S. Environmental Protection Agency. Mention of trade names or commercial products does not constitute endorsement or recommendation for use. The authors would like to thank Dr. Jim Kaldy and Dr. Jeffrey Welker for the isotopic data from Newport and Alsea, respectively, Dr. Julia Jones, Dr. Sharon Bywater-Reyes, and Dr. Fred Swanson for insightful discussions, and to Dr. Stephen Good for comments on an earlier version of this work. Additional thanks to the City of Corvallis for granting access to water samples in Rock Creek, to the OSU Research Forest for providing as access to meteorological data. The isotopic data collected will be submitted to the IAEA Global Network of Isotopes in Rivers.

REFERENCES

Araguas-Araguas, L., Froehlich, K., & Rozanski, K. (2000). Deuterium and oxygen-18 isotope composition of precipitation and atmospheric moisture. *Hydrological Processes*, *14*, 1341–1355. doi:10.1002/1099-1085(20000615)14:8<1341::aid-hyp983>3.0.co;2-z

Baldwin, W. M. (1964). *Geology of Oregon*. University of Oregon.

Benjamin, L., Knobel, L. L., Hall, L. F., Cecil, L. D., Green, J. R. (2005). Development of a local meteoric water line for southeastern Idaho, western Wyoming, and south-central Montana. In: Scientific Investigations Report.

Bershaw, J., Penny, S. M., & Garzione, C. N. (2012). Stable isotopes of modern water across the Himalaya and eastern Tibetan Plateau: Implications for estimates of paleoelevation and paleoclimate. *Journal of Geophysical Research-Atmospheres*, *117*, n/a-n/a. doi:10.1029/2011JD016132.

Bershaw, J., Saylor, J. E., Garzione, C. N., Leier, A., & Sundell, K. E. (2016). Stable isotope variations (delta O-18 and delta D) in modern waters across the Andean Plateau. *Geochimica et Cosmochimica Acta*, *194*, 310–324. doi:10.1016/j.gca.2016.08.011

Biggs, T. W., Lai, C. T., Chandan, P., Lee, R. M., Messina, A., Lesher, R. S., & Khatoon, N. (2015). Evaporative fractions and elevation effects on stable isotopes of high elevation lakes and streams in arid western Himalaya. *Journal of Hydrology*, *522*, 239–249. doi:10.1016/j.jhydrol.2014.12.023

Blumstock, M., Tetzlaff, D., Malcolm, I. A., Nuetzmann, G., & Soulsby, C. (2015). Baseflow dynamics: Multi-tracer surveys to assess variable groundwater contributions to montane streams under low flows. *Journal of Hydrology*, *527*, 1021–1033. doi:10.1016/j.jhydrol.2015.05.019

Brooks, J. R., Wigington, P. J., Phillips, D. L., Comeleo, R., & Coulombe, R. (2012). Willamette River Basin surface water isoscape (delta O-18 and delta H-2): Temporal changes of source water within the river. *Ecosphere*, *3*, 21. doi:10.1890/es11-00338.1

Buttle, J. M., Dillon, P. J., & Eerkes, G. R. (2004). Hydrologic coupling of slopes, riparian zones and streams: An example from the Canadian shield. *Journal of Hydrology*, *287*, 161–177. doi:10.1016/j.jhydrol.2003.09.022

Buttle, J. M., Creed, I. F., & Moore, R. D. (2005). Advances in Canadian forest hydrology, 1999–2003. *Hydrological Processes*, *19*, 169–200. doi:10.1002/hyp.5773

Capell, R., Tetzlaff, D., Hartley, A. J., & Soulsby, C. (2012). Linking metrics of hydrological function and transit times to landscape controls in a heterogeneous mesoscale catchment. *Hydrological Processes*, *26*, 405–420. doi:10.1002/hyp.8139

Condon, L. E., & Maxwell, R. M. (2015). Evaluating the relationship between topography and groundwater using outputs from a continental-scale integrated hydrology model. *Water Resources Research*, *51*, 6602–6621. doi:10.1002/2014wr016774

Craig, H. (1961). Isotopic variations in meteoric waters. *Science*, *133*, 1702–1703. doi:10.1126/science.133.3465.1702

Dansgaard, W. (1964). Stable isotopes in precipitation. *Tellus*, *16*, 436–468. doi:10.1111/j.2153-3490.1964.tb00181.x

Devito, K., Creed, I., Gan, T., Mendoza, C., Petrone, R., Silins, U., & Smerdon, B. (2005). A framework for broad-scale classification of hydrologic response units on the Boreal Plain: Is topography the last thing to consider? *Hydrological Processes*, *19*, 1705–1714. doi:10.1002/hyp.5881

Dutton, A., Wilkinson, B. H., Welker, J. M., Bowen, G. J., & Lohmann, K. C. (2005). Spatial distribution and seasonal variation in 18O/16O of

modern precipitation and river water across the conterminous USA. *Hydrological Processes*, *19*, 4121–4146. doi:10.1002/hyp.5876

Fan, Y., Chen, Y., Li, X., Li, W., & Li, Q. (2015). Characteristics of water isotopes and ice-snowmelt quantification in the Tizinafu River, north Kunlun Mountains, Central Asia. *Quaternary International*, *380–381*, 116–122. doi:10.1016/j.quaint.2014.05.020

Freeze, R. A. (1974). Streamflow generation. *Reviews of Geophysics*, *12*, 627–647. doi:10.1029/RG012i004p00627

Gibson, J. J., Edwards, T. W. D., Birks, S. J., St Amour, N. A., Buhay, W. M., McEachern, P., … Peters, D. L. (2005). Progress in isotope tracer hydrology in Canada. *Hydrological Processes*, *19*, 303–327. doi:10.1002/hyp.5766

Grabs, T., Seibert, J., Bishop, K., & Laudon, H. (2009). Modeling spatial patterns of saturated areas: A comparison of the topographic wetness index and a dynamic distributed model. *Journal of Hydrology*, *373*, 15–23. doi:10.1016/j.jhydrol.2009.03.031

Grayson, R., & Western, A. (2001). Terrain and the distribution of soil moisture. *Hydrological Processes*, *15*, 2689–2690. doi:10.1002/hyp.479

Groning, M., Lutz, H. O., Roller-Lutz, Z., Kralik, M., Gourcy, L., & Poltenstein, L. (2012). A simple rain collector preventing water re-evaporation dedicated for delta O-18 and delta H-2 analysis of cumulative precipitation samples. *Journal of Hydrology*, *448*, 195–200. doi:10.1016/j.jhydrol.2012.04.041

Haitjema, H. M., & Mitchell-Bruker, S. (2005). Are water tables a subdued replica of the topography? *Ground Water*, *43*, 781–786. doi:10.1111/j.1745-6584.2005.00090.x

Hale, V. C., & McDonnell, J. J. (2016). Effect of bedrock permeability on stream base flow mean transit time scaling relations: 1. A multiscale catchment intercomparison. *Water Resources Research*, *52*, 1358–1374. doi:10.1002/2014WR016124

Hale, V. C., McDonnell, J. J., Stewart, M. K., Solomon, D. K., Doolitte, J., Ice, G. G., & Pack, R. T. (2016). Effect of bedrock permeability on stream base flow mean transit time scaling relationships: 2. Process study of storage and release. *Water Resources Research*, *52*, 1375–1397. doi:10.1002/2015wr017660

Heidbuchel, I., Troch, P. A., & Lyon, S. W. (2013). Separating physical and meteorological controls of variable transit times in zero-order catchments. *Water Resources Research*, *49*, 7644–7657. doi:10.1002/2012wr013149

Heidbuechel, I., Troch, P. A., & Lyon, S. W. (2013). Separating physical and meteorological controls of variable transit times in zero-order catchments. *Water Resources Research*, *49*, 7644–7657. doi:10.1002/2012wr013149

Homer, C. G., Dewitz, J. A., Yang, L., Danielson, P., Xian, G., Coulston, J., … Megown, K. (2015). Completion of the 2011 National Land Cover Database for the conterminous United States-representing a decade of land cover change information. *Photogrammetric Engineering and Remote Sensing*, *81*, 345–354.

Jasechko, S., Kirchner, J. W., Welker, J. M., & McDonnell, J. J. (2016). Substantial proportion of global streamflow less than three months old. *Nature Geoscience*, *9*, 126–12+. doi:10.1038/ngeo2636

Jeelani, G., Saravana Kumar, U., & Kumar, B. (2013). Variation of δ18O and δD in precipitation and stream waters across the Kashmir Himalaya (India) to distinguish and estimate the seasonal sources of stream flow. *Journal of Hydrology*, *481*, 157–165. doi:10.1016/j.jhydrol.2012.12.035

Jefferson, A. J. (2011). Seasonal versus transient snow and the elevation dependence of climate sensitivity in maritime mountainous regions. *Geophysical Research Letters*, *38*, n/a-n/a. doi:10.1029/2011GL048346.

Jefferson, A., Grant, G., & Rose, T. (2006). Influence of volcanic history on groundwater patterns on the west slope of the Oregon High Cascades. *Water Resources Research*, *42*. doi:10.1029/2005wr004812

Kendall, C., & McDonnell, J. J. (1998). *Isotope tracers in catchment hydrology*. Elsevier Science B.V.

Klaus, J., & McDonnell, J. J. (2013). Hydrograph separation using stable isotopes: Review and evaluation. *Journal of Hydrology*, *505*, 47–64. doi:10.1016/j.jhydrol.2013.09.006

Koeniger, P., Leibundgut, C., & Stichler, W. (2009). Spatial and temporal characterisation of stable isotopes in river water as indicators of groundwater contribution and confirmation of modelling results; a study of the Weser river, Germany. *Isotopes in Environmental and Health Studies*, *45*, 289–302. doi:10.1080/10256010903356953

Lechler, A. R., & Niemi, N. A. (2011). Controls on the spatial variability of modern meteoric delta o-18: empirical constraints from the Western US and East Asia and implications for stable isotope studies. *American Journal of Science*, *311*, 664–700. doi:10.2475/08.2011.02

Leibowitz, S. G., Wigington, P. J. Jr., Comeleo, R. L., & Ebersole, J. L. (2012). A temperature–precipitation-based model of thirty-year mean snowpack accumulation and melt in Oregon, USA. *Hydrological Processes*, *26*, 741–759. doi:10.1002/hyp.8176

Li, Z., Qi, F., Li, J., Pan, Y., Wang, T., Li, L., … Rui, G. (2015). Environmental significance and hydrochemical processes at a cold alpine basin in the Qilian Mountains. *Environmental Earth Sciences*, *73*, 4043–4052. doi:10.1007/s12665-014-3689-4

Martinelli, L. A., Gat, J. R., De Camargo, P. B., Lara, L. L., & Ometto, J. P. H. B. (2004). The Piracicaba river basin: Isotope hydrology of a tropical river basin under anthropogenic stress. *Isotopes in Environmental and Health Studies*, *40*, 45–56. doi:10.1080/10256010310001652016

Martinez, J. L., Raiber, M., & Cox, M. E. (2015). Assessment of groundwater–surface water interaction using long-term hydrochemical data and isotope hydrology: Headwaters of the Condamine River, Southeast Queensland, Australia. *Science of the Total Environment*, *536*, 499–516. doi:10.1016/j.scitotenv.2015.07.031

Mattson, K., Runyon, J., Fernald, S., Gallagher, A., Johnson, R., Snyder, K., … Zybach, R. (1999). *Marys River watershed preliminary assessment*. (pp. 158). Ecosystems Northwest.

Maxwell, R. M., Condon, L. E., Kollet, S. J., Maher, K., Haggerty, R., & Forrester, M. M. (2016). The imprint of climate and geology on the residence times of groundwater. *Geophysical Research Letters*, *43*, 701–708. doi:10.1002/2015gl066916

McDonnell, J. J. (2003). Where does water go when it rains? Moving beyond the variable source area concept of rainfall-runoff response. *Hydrological Processes*, *17*, 1869–1875. doi:10.1002/hyp.5132

McDonnell, J. J., Sivapalan, M., Vache, K., Dunn, S., Grant, G., Haggerty, R., … Weiler, M. (2007). Moving beyond heterogeneity and process complexity: A new vision for watershed hydrology. *Water Resources Research*, 43.

McDonnell, J. J., McGuire, K., Aggarwal, P., Beven, K. J., Biondi, D., Destouni, G., … Wrede, S. (2010). How old is streamwater? Open questions in catchment transit time conceptualization, modelling and analysis. *Hydrological Processes*, *24*, 1745–1754. doi:10.1002/hyp.7796

McGlynn, B. L., McDonnel, J. J., & Brammer, D. D. (2002). A review of the evolving perceptual model of hillslope flowpaths at the Maimai catchments, New Zealand. *Journal of Hydrology*, *257*, 1–26. doi:10.1016/S0022-1694(01)00559-5

McGuire, K. J., & McDonnell, J. J. (2006). A review and evaluation of catchment transit time modeling. *Journal of Hydrology*, *330*, 543–563.

McGuire, K. J., McDonnell, J. J., Weiler, M., Kendall, C., McGlynn, B. L., Welker, J. M., & Seibert, J. (2005). The role of topography on catchment-scale water residence time. *Water Resources Research*, *41*, W05002-W05002. doi:10.1029/2004WR003657.

Moore, R. D., & Thompson, J. C. (1996). Are water table variations in a shallow forest soil consistent with the TOPMODEL concept? *Water Resources Research*, *32*, 663–669. doi:10.1029/95wr03487

Mountain, N., James, A. L., & Chutko, K. (2015). Groundwater and surface water influences on streamflow in a mesoscale Precambrian Shield catchment. *Hydrological Processes*, *29*, 3941–3953. doi:10.1002/hyp.10590

Négrel, P., Petelet-Giraud, E., & Millot, R. (2016). Tracing water cycle in regulated basin using stable δ18O–δ2H isotopes: The Ebro river basin

(Spain). *Chemical Geology*, *422*, 71–81. doi:10.1016/j.chemgeo.2015.12.009

O'Connor, J. E., Mangano, J. F., Anderson, S. W., Wallick, J. R., Jones, K. L., & Keith, M. K. (2014). Geologic and physiographic controls on bed-material yield, transport, and channel morphology for alluvial and bedrock rivers, western Oregon. *Geological Society of America Bulletin*, *126*, 377–397. doi:10.1130/b30831.1

Ogrinc, N., Kanduč, T., Stichler, W., & Vreča, P. (2008). Spatial and seasonal variations in δ18O and δD values in the River Sava in Slovenia. *Journal of Hydrology*, *359*, 303–312. doi:10.1016/j.jhydrol.2008.07.010

Parajka, J., Viglione, A., Rogger, M., Salinas, J. L., Sivapalan, M., & Blöschl, G. (2013). Comparative assessment of predictions in ungauged basins – part 1: Runoff-hydrograph studies. *Hydrology and Earth System Sciences*, *17*, 1783–1795. doi:10.5194/hess-17-1783-2013

Patil, S. D., Wigington, P. J., Leibowitz, S. G., Sproles, E. A., & Comeleo, R. L. (2014). How does spatial variability of climate affect catchment streamflow predictions? *Journal of Hydrology*, *517*, 135–145. doi:10.1016/j.jhydrol.2014.05.017

Payn, R. A., Gooseff, M. N., McGlynn, B. L., Bencala, K. E., & Wondzell, S. M. (2012). Exploring changes in the spatial distribution of stream baseflow generation during a seasonal recession. *Water Resources Research*, *48*. doi:10.1029/2011wr011552

Peng, T.-R., Chen, K.-Y., Zhan, W.-J., Lu, W.-C., & Tong, L.-T. J. (2015). Use of stable water isotopes to identify hydrological processes of meteoric water in montane catchments. *Hydrological Processes*, *29*, 4957–4967. doi:10.1002/hyp.10557

Pereira, R., Bovolo, C. I., Forsythe, N., Pedentchouk, N., Parkin, G., & Wagner, T. (2014). Seasonal patterns of rainfall and river isotopic chemistry in northern Amazonia (Guyana): From the headwater to the regional scale. *Journal of South American Earth Sciences*, *52*, 108–118. doi:10.1016/j.jsames.2014.02.005

Poage, M. A., & Chamberlain, C. P. (2001). Empirical relationships between elevation and the stable isotope composition of precipitation and surface waters: Considerations for studies of paleoelevation change. *American Journal of Science*, *301*, 1–15. doi:10.2475/ajs.301.1.1

Pu, T., He, Y., Zhu, G., Zhang, N., Du, J., & Wang, C. (2013). Characteristics of water stable isotopes and hydrograph separation in Baishui catchment during the wet season in Mt.Yulong region, south western China. *Hydrological Processes*, *27*, 3641–3648. doi:10.1002/hyp.9479

Rhea, S. (1993). Geomorphic observations of rivers in the Oregon Coast Range from a regional reconnaissance perspective. *Geomorphology*, *6*, 135–150. doi:10.1016/0169-555X(93)90043-2

Rodgers, P., Soulsby, C., & Waldron, S. (2005). Stable isotope tracers as diagnostic tools in upscaling flow path understanding and residence time estimates in a mountainous mesoscale catchment. *Hydrological Processes*, *19*, 2291–2307. doi:10.1002/hyp.5677

Rose, S. (1996). Temporal environmental isotopic variation within the Falling Creek (Georgia) watershed: Implications for contributions to streamflow. *Journal of Hydrology*, *174*, 243–261. doi:10.1016/0022-1694(95)02767-x

Rugel, K., Golladay, S. W., Jackson, C. R., & Rasmussen, T. C. (2016). Delineating groundwater/surface water interaction in a karst watershed: Lower Flint River Basin, southwestern Georgia, USA. *Journal of Hydrology: Regional Studies*, *5*, 1–19. doi:10.1016/j.ejrh.2015.11.011

Scholl, M. A., Shanley, J. B., Murphy, S. F., Willenbring, J. K., Occhi, M., & González, G. (2015). Stable-isotope and solute-chemistry approaches to flow characterization in a forested tropical watershed, Luquillo Mountains, Puerto Rico. *Applied Geochemistry*, *63*, 484–497. doi:10.1016/j.apgeochem.2015.03.008

Schulte, P., van Geldern, R., Freitag, H., Karim, A., Négrel, P., Petelet-Giraud, E., … Barth, J. A. C. (2011). Applications of stable water and carbon isotopes in watershed research: Weathering, carbon cycling, and water balances. *Earth-Science Reviews*, *109*, 20–31. doi:10.1016/j.earscirev.2011.07.003

Séguis, L., Kamagaté, B., Favreau, G., Descloitres, M., Seidel, J. L., Galle, S., … Wubda, M. (2011). Origins of streamflow in a crystalline basement catchment in a sub-humid Sudanian zone: The Donga basin (Benin, West Africa): Inter-annual variability of water budget. *Journal of Hydrology*, *402*, 1–13. doi:10.1016/j.jhydrol.2011.01.054

Sheppard, S. M. F., & Gilg, H. A. (1996). Stable isotope geochemistry of clay minerals; the story of sloppy, sticky, lumpy and tough, Cairns-Smith (1971). *Clay Minerals*, *31*, 1–24.

Singh, N. K., Emanuel, R. E., & McGlynn, B. L. (2016). Variability in isotopic composition of base flow in two headwater streams of the southern Appalachians. *Water Resources Research*, *52*, 4264–4279. doi:10.1002/2015wr018463

Soulsby, C., Malcolm, R., Helliwell, R., Ferrier, R. C., & Jenkins, A. (2000). Isotope hydrology of the Allt a' Mharcaidh catchment, Cairngorms, Scotland: Implications for hydrological pathways and residence times. *Hydrological Processes*, *14*, 747–762. doi:10.1002/(SICI)1099-1085(200003)14:4<747::AID-HYP970>3.0.CO;2-0

Soulsby, C., Birkel, C., Geris, J., Dick, J., Tunaley, C., & Tetzlaff, D. (2015). Stream water age distributions controlled by storage dynamics and nonlinear hydrologic connectivity: Modeling with high-resolution isotope data. *Water Resources Research*, *51*, 7759–7776. doi:10.1002/2015wr017888

Speed, M., Tetzlaff, D., Hrachowitz, M., & Soulsby, C. (2011). Evolution of the spatial and temporal characteristics of the isotope hydrology of a montane river basin. *Hydrological Sciences Journal*, *56*, 426–442. doi:10.1080/02626667.2011.561208

Sprenger, M., Seeger, S., Blume, T., & Weiler, M. (2016). Travel times in the vadose zone: Variability in space and time. *Water Resources Research*, *52*, 5727–5754. doi:10.1002/2015WR018077

Tetzlaff, D., Uhlenbrook, S., Eppert, S., & Soulsby, C. (2008). Does the incorporation of process conceptualization and tracer data improve the structure and performance of a simple rainfall-runoff model in a Scottish mesoscale catchment? *Hydrological Processes*, *22*, 2461–2474.

U.S. Census Bureau PD. (2015). Annual estimates of the resident population: April 1, 2010 to July 1, 2015 Source: http://factfinder.census.gov/faces/tableservices/jsf/pages/productview.xhtml?src=bkmk.

Vespasiano, G., Apollaro, C., De Rosa, R., Muto, F., Larosa, S., Fiebig, J., … Marini, L. (2015). The Small Spring Method (SSM) for the definition of stable isotope–elevation relationships in Northern Calabria (Southern Italy). *Applied Geochemistry*, *63*, 333–346. doi:10.1016/j.apgeochem.2015.10.001

Wagener, T., & Montanari, A. (2011). Convergence of approaches toward reducing uncertainty in predictions in ungauged basins. *Water Resources Research*, *47*, . doi:10.1029/2010WR009469.n/a-n/a

Walker, G. W., MacLeod, N. S. (2002). Spatial digital database for the geologic map of Oregon. Open-File Report 03-67. U.S. Geological Survey.

Wang, N., Zhang, S., He, J., Pu, J., Wu, X., & Jiang, X. (2009). Tracing the major source area of the mountainous runoff generation of the Heihe River in Northwest China using stable isotope technique. *Chinese Science Bulletin*, *54*, 2751–2757. doi:10.1007/s11434-009-0505-8

Wassenaar, L. I., Van Wilgenburg, S. L., Larson, K., & Hobson, K. A. (2009). A groundwater isoscape (δD, δ18O) for Mexico. *Journal of Geochemical Exploration*, *102*, 123–136. doi:10.1016/j.gexplo.2009.01.001

Wassenaar, L. I., Athanasopoulos, P., & Hendry, M. J. (2011). Isotope hydrology of precipitation, surface and ground waters in the Okanagan Valley, British Columbia, Canada. *Journal of Hydrology*, *411*, 37–48. doi:10.1016/j.jhydrol.2011.09.032

Wiley, T. J. (2008). Preliminary geologic maps of the Corvallis, Wren, and Marys peak 7.5′ quadrangles, Benton, Lincoln, and Linn counties, Oregon. State of Oregon Department of Geology and Mineral Industries, pp: 10.

Williams, A. E., & Rodoni, D. P. (1997). Regional isotope effects and application to hydrologic investigations in southwestern California. *Water Resources Research*, *33*, 1721–1729. doi:10.1029/97WR01035

Yadav, M., Wagener, T., & Gupta, H. (2007). Regionalization of constraints on expected watershed response behavior for improved predictions in ungauged basins. *Advances in Water Resources*, *30*, 1756–1774. doi:10.1016/j.advwatres.2007.01.005

Yonge, C. J., Goldenberg, L., & Krouse, H. R. (1989). An isotope study of water bodies along a traverse of southwestern Canada. *Journal of Hydrology*, *106*, 245–255. doi:10.1016/0022-1694(89)90075-9

Zhang, Z., Wagener, T., Reed, P., & Bhushan, R. (2008). Reducing uncertainty in predictions in ungauged basins by combining hydrologic indices regionalization and multiobjective optimization. *Water Resources Research*, *44*, n/a-n/a. doi:10.1029/2008WR006833.

How to cite this article: Nickolas LB, Segura C, Brooks JR. The influence of lithology on surface water sources. *Hydrological Processes*. 2017. https://doi.org/10.1002/hyp.11156